

Article

Contribution of Endothelial Laminin-Binding Integrins to Cellular Processes Associated with Angiogenesis

Hao Xu and Susan E. LaFlamme *

Department of Regenerative and Cancer Cell Biology, Albany Medical College, 47 New Scotland Ave., Albany, NY 12208, USA; haoxu1@upenn.edu

* Correspondence: laflams@amc.edu

Abstract: Endothelial cells engage extracellular matrix and basement membrane components through integrin-mediated adhesion to promote angiogenesis. Angiogenesis involves the sprouting of endothelial cells from pre-existing vessels, their migration into surrounding tissue, the upregulation of angiogenesis-associated genes, and the formation of new endothelial tubes. To determine whether the endothelial laminin-binding integrins, $\alpha 6\beta 4$, and $\alpha 3\beta 1$ contribute to these processes, we employed RNAi technology in organotypic angiogenesis assays, as well in migration assays, in vitro. The endothelial depletion of either $\alpha 6\beta 4$ or $\alpha 3\beta 1$ inhibited endothelial sprouting, indicating that these integrins have non-redundant roles in this process. Interestingly, these phenotypes were accompanied by overlapping and distinct changes in the expression of angiogenesis-associated genes. Lastly, depletion of $\alpha 6\beta 4$, but not $\alpha 3\beta 1$, inhibited migration. Taken together, these results suggest that laminin-binding integrins regulate processes associated with angiogenesis by distinct and overlapping mechanisms.

Keywords: integrins; laminin; angiogenesis; gene expression



Citation: Xu, H.; LaFlamme, S.E. Contribution of Endothelial Laminin-Binding Integrins to Cellular Processes Associated with Angiogenesis. *Cells* **2022**, *11*, 816. <https://doi.org/10.3390/cells11050816>

Academic Editor: Daniel Bouvard

Received: 20 January 2022

Accepted: 23 February 2022

Published: 26 February 2022

Publisher's Note: MDPI stays neutral with regard to jurisdictional claims in published maps and institutional affiliations.



Copyright: © 2022 by the authors. Licensee MDPI, Basel, Switzerland. This article is an open access article distributed under the terms and conditions of the Creative Commons Attribution (CC BY) license (<https://creativecommons.org/licenses/by/4.0/>).

1. Introduction

Angiogenesis contributes to both normal and pathological processes, including tissue repair, cancer progression, and inflammation [1,2]. Angiogenesis is a multistep process that involves the sprouting of endothelial cells from the pre-existing vasculature, which then form endothelial tubes that anastomose with one another to form new vascular networks. Although many mechanisms and regulatory pathways have been identified, a further understanding of the underlying mechanisms that regulate specific aspects of new vessel formation remains an important objective.

At the onset of angiogenesis, endothelial cells interact with proteins present in the extracellular matrix, some of which are provided by other cell types, such as those present in the provisional matrix during tissue repair [3,4]. Endothelial cells themselves also secrete matrix proteins including fibronectin and the basement membrane components, laminin-411 and laminin-511. The interaction of endothelial cells with these adhesion proteins using members of the integrin family of adhesion receptors contributes to the formation and stabilization of endothelial tubes [3,5–9].

Endothelial cells express several integrin heterodimers, including the three laminin-binding receptors $\alpha 3\beta 1$, $\alpha 6\beta 1$, and $\alpha 6\beta 4$, which are known to bind laminin-511 [3,9–11]. Global deletion of the $\alpha 3$ subunit (*Itga3*), the $\alpha 6$ subunit (*Itga6*), or the $\beta 4$ subunit gene (*Itgb4*) in mice demonstrated that integrins $\alpha 3\beta 1$, $\alpha 6\beta 1$, and $\alpha 6\beta 4$ are not required for developmental angiogenesis [12–17]. To study the role of these integrins during angiogenesis in the adult, several labs have used the conditional endothelial deletion of either the integrin $\alpha 3$ subunit, the $\alpha 6$ subunit, or the $\beta 4$ integrin subunit gene. The loss of expression of the $\alpha 3\beta 1$ integrin has led to enhanced pathological angiogenesis, suggesting that endothelial $\alpha 3\beta 1$ functions to inhibit angiogenesis [15]. The loss of $\alpha 6$ integrins has been reported to

either promote or inhibit angiogenesis, depending upon whether $\alpha 6$ alleles were targeted by the expression of either a Tie1- or Tie2-driven Cre recombinase [16–19]. The mechanisms responsible for these disparate phenotypes are not fully understood; however, the phenotype of mice expressing the Tie2-driven Cre recombinase exhibited defects due to the loss of the expression of $\alpha 6$ integrins not only in endothelial cells, but also in macrophage and endothelial progenitors [16–19]. It has been difficult to distinguish contributions from $\alpha 6\beta 1$ and $\alpha 6\beta 4$ during angiogenesis, as the integrin $\beta 1$ subunit dimerizes with multiple α subunits in endothelial cells, making it difficult to discern functions specific to $\alpha 6\beta 1$ when $\alpha 6\beta 4$ is also expressed. Mouse genetic studies examining the effect of Tie2-dependent deletion of the $\beta 4$ subunit have not focused on angiogenesis per se; however, these studies have identified a role for $\alpha 6\beta 4$ in hypoxia-induced vessel remodeling and in promoting endothelial barrier function in the brain vasculature in response to inflammation [20,21]. Others have demonstrated that $\alpha 6\beta 4$ is expressed by angiogenic vessels and that the global deletion of the signaling portion of the $\beta 4$ subunit cytoplasmic domain inhibited tumor angiogenesis [22]. Nonetheless, the contribution of endothelial $\alpha 6\beta 4$ to angiogenesis has not been directly examined in the adult, and is complicated by the disparate reports of the restricted expression of the $\alpha 6\beta 4$ integrin to a subset of endothelial cells [20,22,23].

In the current study, we dissected the roles of individual laminin-binding integrins in cellular processes that contribute to angiogenesis. We employed RNAi technology together with organotypic angiogenesis assays—which model angiogenesis in an ECM environment, similar to that present during tissue repair [24–26]—in addition to transwell migration assays. Using these assays, we previously demonstrated that endothelial cells secrete both laminin-411 and laminin-511 during the formation of endothelial tubes [7]. We also showed that the expression of these laminin isoforms, as well as $\alpha 6$ integrins, are required for these processes [7]. In addition, we implicated the $\alpha 6$ -dependent regulation of the angiogenesis-associated gene angiopoitin-2 (ANGPT2) and the chemokine receptor, CXCR4 [7]. However, our previous studies did not distinguish contributions from $\alpha 6\beta 1$ or $\alpha 6\beta 4$ or whether the laminin-binding integrin $\alpha 3\beta 1$ also contributes to endothelial morphogenesis in organotypic angiogenesis assays. Our current data suggest that the $\alpha 3\beta 1$ and $\alpha 6\beta 4$ integrins contribute to endothelial sprouting by non-redundant mechanisms. Moreover, gene expression analyses indicate that these integrins contribute to the expression of distinct but overlapping sets of angiogenesis-associated genes. To our knowledge, our study is the first to examine the contribution of laminin-binding integrins to the regulation of a set of previously identified angiogenesis-associated genes.

2. Materials and Methods

2.1. Immunofluorescence Microscopy

2.1.1. Immunostaining

Murine tissue: Murine ears were separated into dorsal and ventral layers and the epidermis subsequently removed with the blunt end of a pair of forceps in EDTA. Whole-mount murine retinas, ears and cryo-sectioned skin were fixed with 4% PFA for 30 min, permeabilized with 0.5% Triton X-100 in PBS for 30 min, and then blocked with 2% BSA and 0.1% saponin in PBS overnight at 4 °C. Antibodies were diluted in 2% BSA and 0.1% saponin in PBS and incubated with tissue for 48 h at 4 °C. Samples were then washed 4× with 0.1% saponin in PBS at RT over the course of 24 h, then incubated overnight with the appropriate secondary antibodies (1:1000 dilution) at 4 °C. Following secondary antibody staining, samples were washed 4× with 0.1% saponin in PBS at RT over the course of 24 h and mounted with SlowFade Gold antifade reagent (ThermoFisher, Waltham, MA, USA). See Table S1 for antibody information. **Bead-sprout and planar co-culture assays:** Bead-sprout and planar co-cultures were fixed with 4% PFA (Electron Microscopy Sciences, Hatfield, PA, USA) for 15 min, permeabilized with 0.5% Triton X-100 in PBS for 15 min, and then blocked with 2% BSA in PBST (PBS + 0.1% Tween20) for 1 h at RT. In the case of bead-sprout assays, fibroblasts were removed using trypsin-EDTA Solution 10× (59418C, Sigma Aldrich, St. Louis, MO, USA) prior to fixation and imaging. Antibodies were diluted

in 2% BSA in PBST, and incubated with cells overnight at 4 °C. Samples were then washed 4× with PBST at RT over the course of 4 h, then incubated for 1 h with the appropriate secondary antibodies (1:1000 dilution). Following secondary antibody staining, samples were washed 3× with PBST at RT for 1 h and mounted with SlowFade Gold antifade reagent (ThermoFisher). See Table S1 for antibody information.

2.1.2. Microscopy

Most samples were analyzed using a Nikon inverted TE2000-E microscope equipped with phase contrast and epifluorescence, a digital CoolSNAP HQ camera, a Prior ProScanII motorized stage, and a Nikon C1 confocal system, using EZC1-3.90 and NIS-Elements-AR acquisition software (Nikon, Melville, NY, USA). Images were acquired with Plan Fluor 4×/0.13, Plan Fluor 10×/0.30, Plan Fluor ELWD 20×/0.45, Plan Apo 40×/1.0 oil, and Plan Apo 100×/1.4 oil objectives, and analyzed with NIS elements (Nikon). Contrast and/or brightness were adjusted for some images to assist in visualization. To image murine skin at high resolution, a Zeiss LSM 880 confocal microscope system with AiryScan detector and a FAST Airyscan module mounted on an AxioObserver (Carl Zeiss, Inc, Peabody, MA, USA) was used. The LSM 880 confocal detection system had 34 spectral-detection channels consisting of a cooled 32 element GaAsP detector array with two flanking photomultiplier tubes (PMTs). Wavelength separation was achieved using high-efficiency grating; maximum spectral resolution was 3 nm over a 286 nm range (410 to 696 nm). Objective lenses: 10×|0.45 NA (air), 20×/0.8 NA DIC, 25×|0.8 multi-immersion DIC, 40×|1.4 NA W DIC, 63×|1.4 NA DIC oil, C-Apochromat 40×/1.2 W/korr FCS, Plan-Apochromat 63×/1.4 NA oil DIC ELYRA. Six single-photon-excitation laser lines were available: 405, 458, 488, 514, 561 and 633 nm.

2.1.3. Analysis of Sprouting

Sprout lengths in bead-sprout assays were measured by tracing each sprout using NIS elements (Nikon), and sprouts per bead were counted manually.

2.2. Cell Culture

Human umbilical vein endothelial cells (HUVECs) were from Lonza (Allendale, NJ, USA) and were cultured in in EGM-2 (Lonza, Walkersville, MD, USA, #CC-3162), and used between passages 2–6. Adult human dermal fibroblasts (HDFs) were isolated and characterized as previously described [27,28]; they were generously provided by Dr. Livingston Van De Water (Albany Medical College, Albany, NY, USA) and used between passages 8–14. Human embryonic kidney epithelial 293FT cells (HEK293FT) were a kind gift from Dr. Alejandro Pablo Adam (Albany Medical College). HDFs and HEK293FT cells were cultured in DMEM (Sigma Aldrich #D6429) containing 10% FBS (Atlanta Biologicals, Flowery Branch, GA, USA), 100 units/mL penicillin (Life Technologies, Carlsbad, CA, USA), 100 µg/mL streptomycin (Life Technologies, Carlsbad, CA, USA), and 2.92 µg/mL L-glutamine (GE LifeSciences, Marlborough, MA, USA). All cells were cultured at 37 °C in 5% CO₂.

2.3. Organotypic Culture Assays

2.3.1. Bead-Sprout Assay

To study endothelial sprouting, we employed the bead-sprout assay as described by Nakatsu and Hughes [26]. Cytodex 3 beads (GE) were coated at ~1000 HUVECs per bead inside of a 2 mL microcentrifuge tube for 4 h at 37 °C, mixed gently by inverting the tubes every 20 min, transferred to a T25 flask and incubated at 37 °C, overnight. Beads were then washed 3× with EGM-2 medium and re-suspended in PBS containing 3 mg/mL of fibrinogen (Sigma Aldrich, #F8630) and 0.15 U/mL of aprotinin (Sigma, #A6279). Thrombin (Sigma, #T4648) was added at a final concentration of 0.125 U/mL and the mixture was plated in wells of an 8-well slide (Corning, Corning, NY, USA #3-35411). The mixture was allowed to clot for 30 min at 37 °C. HDFs were then added to the top surface of the fibrin gel

in EGM-2 medium at a concentration of 30,000 cells per well. The formation of sprouts and sprout lengths were assayed by either immunofluorescence or phase-contrast microscopy.

2.3.2. Planar Co-Culture

As one organotypic culture, we utilized the planar co-culture model developed by Bishop and colleagues [24] and modified by the Pumiglia laboratory [25]. This model reconstitutes some of the complex interactions that occur during angiogenesis among endothelial cells, the ECM and supporting cells. To set up the co-culture, HDFs were seeded in tissue culture dishes with or without glass coverslips and cultured to confluence. The medium was changed to EGM-2. HUVECs were then seeded 16 h later at a density of 20,000 cells per 9 cm² and cultured up to 10 days. Endothelial morphogenesis and $\alpha 6\beta 4$ expression were analyzed by immunofluorescence microscopy.

2.4. siRNA

HUVECs were plated in 6-well tissue-culture plates and transfected with siRNA at a 50 nM concentration with RNAiMAX (ThermoFisher) using the protocol provided by the manufacturer. HUVECs transfected with siRNA were assayed for knockdown and used in migration assays 48 h after transfection. For bead-sprout assays (described above) HUVECs were transfected with siRNA during bead coating and assayed for knockdown at the end of experiment. Sources and nucleotide sequences of siRNAs used in this study are provide in Table S2.

2.5. Inducible shRNA

Doxycycline-inducible lentiviral (SMART) vectors harboring shRNAs targeting the $\alpha 3$ integrin subunit or a non-targeting (NT) shRNA were purchased from Dharmacon (Lafayette, CO, USA). Lentiviruses were produced by co-transfection of HEK293FT cells with the shRNA expression vector together with the packaging plasmid, psPAX2, coding for Gag, Pol, Rev, Tat (#12260, Addgene, Watertown, MA, USA); and the envelope plasmid, pMD2.G, coding for VSV-G (#12259, Addgene, Watertown, MA, USA). HUVECs were transduced with filtered viral supernatant plus 8 $\mu\text{g}/\text{mL}$ polybrene. Cells were induced with doxycycline (100 ng/mL) for 48 h to insure efficient knockdown of $\alpha 3$ expression. Nucleotide sequences of shRNAs used in this study are provided in Table S2.

2.6. Quantitative PCR (qPCR)

TRIzol (ThermoFisher) was used to isolate RNA from siRNA transfected HUVECs, as well as HUVECs expressing shRNAs. Extraction of RNA from bead-sprout assays (described above) using TRIzol was performed after the removal of HDFs with trypsin-EDTA Solution 10 \times (Sigma #59418C). cDNA was synthesized with iScript Reverse Transcription Supermix (BioRad, Hercules, CA, USA) using 1 μg of RNA. Equal amounts of cDNA were used in qPCR reactions performed with iQ SYBR Green Supermix (BioRad, Hercules, CA, USA). PCR primers were pre-designed by, and purchased from, Sigma Aldrich or Integrated DNA Technologies, as indicated in Table S3, together with their nucleotide sequences.

2.7. Western Blotting

Western blotting was used to confirm RNAi-induced knockdown. Cells were lysed in mRIPA buffer (50 mM Tris pH 7.4, 1% NP-40, 0.25% Na Deoxycholate, 150 mM NaCl, 1 mM EDTA) containing both phosphatase (Sigma, #4906837001) and protease inhibitor cocktails (ThermoFisher, 78440, Waltham, MA, USA). Equal amounts of protein (20 to 40 μg) were separated by SDS-PAGE and transferred to nitrocellulose for antibody probing. Imaging was performed with a ChemiDoc XRS+ (BioRad) and quantitation with Image Lab (BioRad). See Table S1 for antibody information.

2.8. Migration

HUVECs were used in migration assays 48 h post-transfection with siRNA, or 48 h post-treatment with doxycycline (100 ng/mL) to induce the expression of SMART Vector shRNAs. After overnight culture in serum-free EGM-2 medium, fifty thousand cells were seeded, in triplicate, into three wells of two separate 24-well plates, one with and without transwells. Serum-containing EGM-2 was then added to the lower chamber. Following an incubation for 4 h at 37 °C in 5% CO₂, transwells were fixed with 4% PFA (Electron Microscopy Sciences). Cells that had not migrated through the filter were gently removed with cotton swabs before staining with DAPI. The lower membrane was imaged with a 4× objective and density quantified using ImageJ (NIH). Cell seeding efficiency was determined by performing toluidine blue assays in the 24-well plates. These assays were performed by fixing cells with 70% ethanol at room temperature for 1 h, followed by a wash with dH₂O and staining with 0.05% toluidine blue at room temperature for an additional 2 h. After the wash with dH₂O, toluidine blue was extracted with 10% acetic acid at 0.3 mL/well and absorbance measured at 650 nm, using 405 nm as reference on a Synergy2 microplate reader (BioTek Instruments, Winooski, VT, USA). An empty well was processed the same way and used for baseline. Migration efficiency was determined by dividing DAPI density by absorbance.

2.9. Animal Experiments

All animal experiments and procedures were performed in accordance with the Albany Medical College Institutional Animal Care and Use Committee (IACUC) regulations; they were performed in accordance with protocols 18-05003 and 18-07001, approved by the Albany Medical College IACUC. Adult murine retinas and ears were harvested from both male and female C57BL/6 mice between the ages of 8–12 weeks. Adult murine skins were harvested from male and female C57BL/6 mice expressing the transgenes: LSL-tdTomato and VE-Cadherin-driven CreERT2. Cre recombinase activity was induced via oral gavage of 10 µg/g of tamoxifen per day for 5 days.

2.10. Statistical Analysis

Statistical analysis was performed with GraphPad Prism software using Single-Sample *t*-test or one-way ANOVA, with post-hoc analysis using Dunnett's or Tukey's multiple comparisons tests as indicated in the figure legends. A *p*-value of *p* < 0.05 was considered to be statistically significant.

3. Results

3.1. Integrin $\alpha 6\beta 4$ Is Expressed in Veins and Small Vessels of the Dermis

Previous studies by us and others showed the expression of $\alpha 6\beta 4$ in tumor-associated angiogenic vessels, as well as angiogenic vessels associated with dermal wound repair [22,23]. In contrast, others reported that $\alpha 6\beta 4$ expression is restricted to arterioles [20]. More recently, single-cell RNA sequencing (scRNA-seq) data of vascular cells of the mouse brain and lung indicated that in the brain, $\beta 4$ mRNA is expressed at higher levels in arterial endothelial cells compared to venous and capillary endothelial cells. In contrast in the lung vasculature, $\beta 4$ mRNA was more widely expressed, including in veins and venules, with higher expression in capillary endothelial cells [29]. The recent scRNAseq data motivated us to re-examine the protein expression of $\alpha 6\beta 4$ to determine whether it is expressed by venous endothelial cells, since angiogenesis is associated with the sprouting of vessels from existing venules and capillaries. Since the $\beta 4$ subunit only dimerizes with the $\alpha 6$ subunit [30], analyzing the expression of the $\beta 4$ subunit is a reliable reporter for the expression of $\alpha 6\beta 4$. We examined the expression of $\alpha 6\beta 4$ in vasculatures of the dermis and brain (retinal vasculature) by immunofluorescence microscopy. Consistent with the scRNAseq data, $\alpha 6\beta 4$ was more widely expressed in endothelial cells outside the brain, specifically in the dermis; this includes in small vessels and venules, in addition to some endothelial cells that are positive for α -SMA (Figure 1A–C). In the adult murine

retinal vasculature, which is considered part of the brain vasculature, $\alpha 6\beta 4$ expression is colocalized with strong expression of α -SMA, which is consistent with its expression in arteries/arterioles in the brain (Figure S1). Thus, our results examining the expression $\alpha 6\beta 4$ protein level are consistent with the previously published scRNA-seq results documenting $\beta 4$ RNA expression in endothelial cells from different parts of the vasculature.

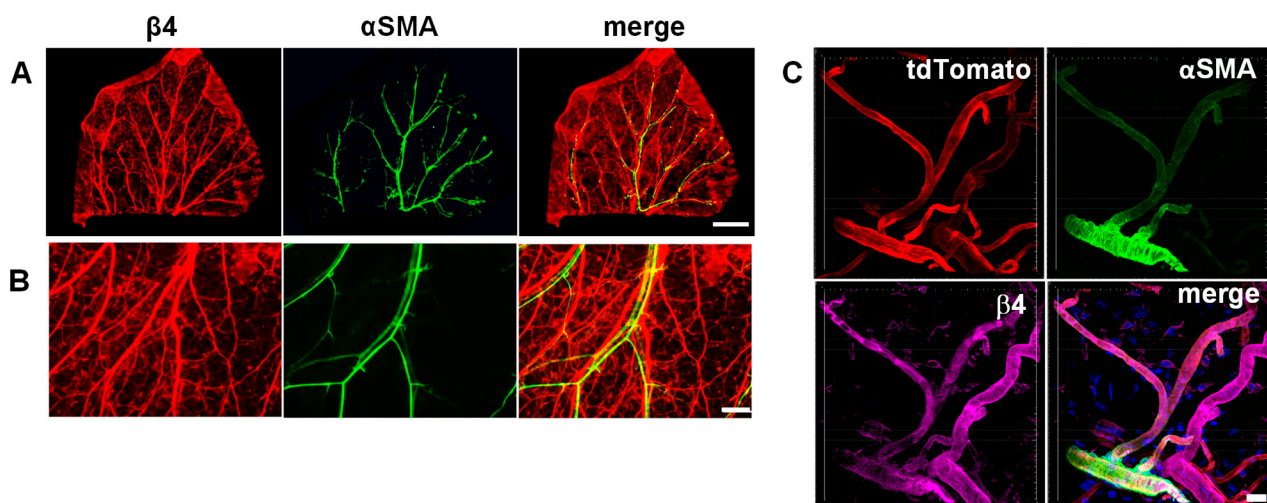


Figure 1. The $\alpha 6\beta 4$ integrin is expressed in veins and venules of the dermal vasculature: (A) immunofluorescence staining of whole-mount mouse ear for α -SMA and $\beta 4$ -integrin subunit. Scale bar = 2 mm; (B) image of $\beta 4$ and α -SMA expression acquired at a higher magnification. Scale bar = 500 μ m; (C) confocal immunofluorescence staining of mouse skin for α -smooth-muscle actin and $\beta 4$ -integrin subunit. Vasculature is identified by tdTomato (red) expression. Image is a maximum projection of acquired z-stack. Arrowhead indicates the location of an arteriole. Scale bar = 20 μ m.

3.2. Integrin $\alpha 6\beta 4$ Promotes Endothelial Morphogenesis

Previous studies have suggested a role for $\alpha 6\beta 4$ in vessel maturation and stability, and its expression has been both positively and negatively associated with angiogenesis [21–23,31]. To determine whether $\alpha 6\beta 4$ expression contributed to processes associated with angiogenesis, we employed an organotypic angiogenesis model (also referred to as a bead-sprout assay), in which cytodex beads coated with endothelial cells (HUVECs) are placed in a fibrin gel overlaid with a confluent layer of dermal fibroblasts, which provide important paracrine signals together with VEGF to promote endothelial sprouting into the gel and subsequent formation of tubes from these sprouts [26,32,33]. Using this model, we previously demonstrated that the expression of $\alpha 6$ integrins is required to promote endothelial sprouting and tube formation; however, we did not determine the specific contributions of $\alpha 6\beta 1$ and $\alpha 6\beta 4$. Since HUVECs express $\alpha 6\beta 4$ on their cell surface (Figure S2), we used the same organotypic co-culture approaches to determine the contribution of $\alpha 6\beta 4$. We analyzed 6-day sprouts of endothelial cells depleted of $\beta 4$, compared to the control. The efficiency of $\beta 4$ mRNA and protein depletion with three distinct targeting siRNAs is shown in Figure 2A,B. Each of the $\beta 4$ -targeting siRNAs significantly inhibited sprouting, as shown in the representative images of 6-day bead sprouts in Figure 2C. Knockdown of the $\beta 4$ subunit, and thus $\alpha 6\beta 4$, with each of these three siRNA sequences resulted in a significant decrease in both sprout length (Figure 2D) and the number of sprouts per bead (Figure 2E). Thus, $\alpha 6\beta 4$ contributes to endothelial sprouting in this organotypic assay.

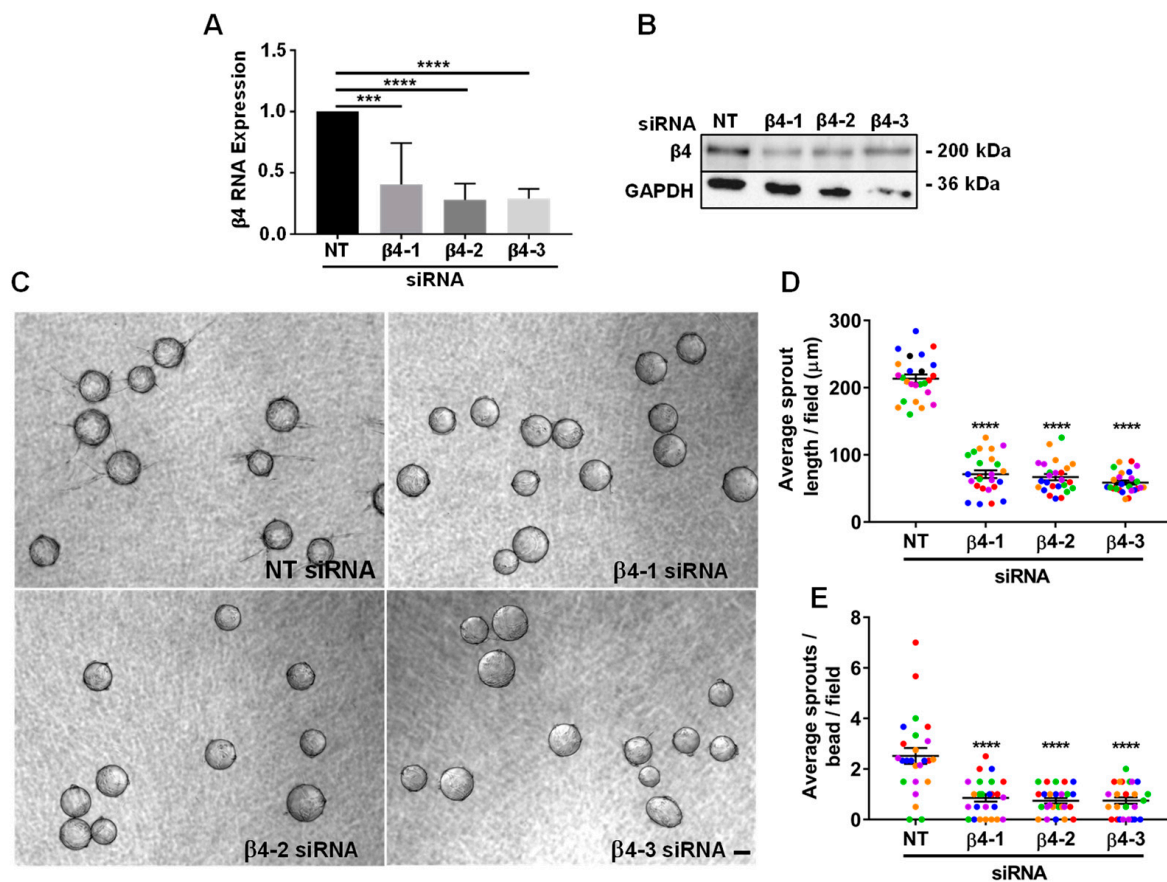


Figure 2. Integrin $\alpha6\beta4$ regulates endothelial morphogenesis: (A) The efficiency of $\beta4$ depletion using 3 siRNA targeting sequences was determined by qPCR. Data were normalized to β -actin and then to non-targeting (NT) control. Plotted is the mean RNA expression \pm s.d. $n = 5$ independent experiments; (B) representative western blot showing the efficiency of $\beta4$ depletion at the protein level. Endothelial cells from the same batches of endothelial cells depleted of the $\beta4$ subunit used in experiments presented in Figure 2 were employed in bead-sprout assays; (C) shown are representative images of 6-day bead sprouts transfected with non-targeting and $\beta4$ -targeting siRNA sequences 1–3. Scale bar = 100 μm ; (D,E) depletion of $\alpha6\beta4$ expression inhibits sprouting. Quantitation of sprout length (top) and number of sprouts (bottom) from 6–8 beads in each of five randomly selected fields in five independent experiments; (D) plotted is the average sprout length per field \pm s.e.m. $n = 25$ fields; (E) quantitation of the average sprouts per bead per field \pm s.e.m. Each independent experiment is represented by a distinct color. Data were analyzed using two-tailed Student's *t*-test. Each independent experiment is represented by a distinct color. *** $p \leq 0.001$, **** $p \leq 0.0001$.

3.3. Integrin $\alpha6\beta4$ Promotes Endothelial Migration

Since cell motility is an important aspect of angiogenesis, we examined the role of $\alpha6\beta4$ in endothelial cell migration. Although we previously demonstrated that $\alpha6$ integrins promote endothelial migration, we did not determine whether $\alpha6\beta4$ contributed to the regulation of cell migration by $\alpha6$ integrins [7]. We inhibited the expression of $\alpha6\beta4$ using RNAi technology. $\beta4$ -depleted endothelial cells did not exhibit defects in proliferation or survival in 2D culture (data not shown), which is consistent with $\beta4$ -depleted endothelial cells in vivo [20,22,23]. We inhibited the expression of $\alpha6\beta4$ by targeting the $\beta4$ subunit with three distinct siRNA-targeting sequences, and measured the effect in transwell migration assays. The depletion of $\beta4$ resulted in a significant reduction in cell migration across gelatin-coated filters (Figure 3A). Importantly, this phenotype was consistent across all three siRNA-targeting sequences, and consistent with previous studies that suggested a role for $\alpha6\beta4$ in the regulation of endothelial cell migration [22]. Although

$\alpha 6\beta 4$ does not bind to gelatin, our previous studies demonstrated that these endothelial cells secrete their own laminin substrates. Thus, endothelial cells are similar to epithelial cells, which secrete their own laminin for migration [34–36].

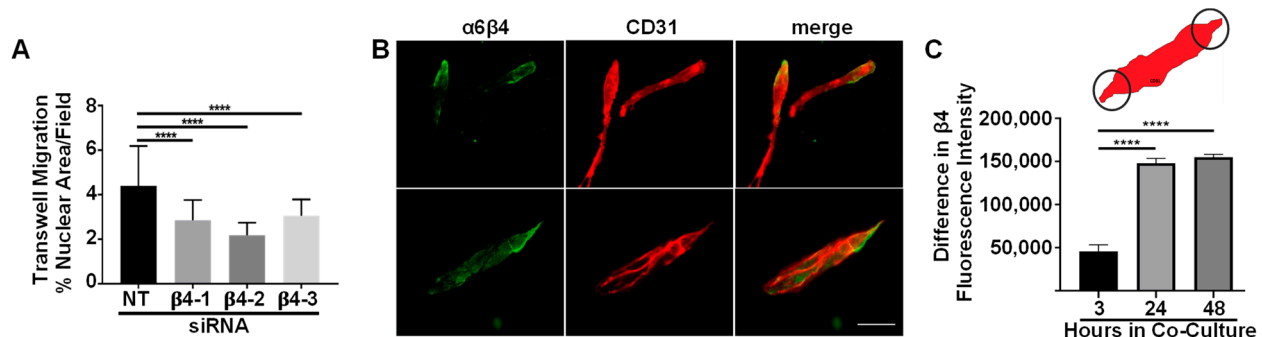


Figure 3. Depletion of $\alpha 6\beta 4$ reduces endothelial cell migration: (A) Analysis of nuclear staining in transwell migration assays with non-targeting (NT) or $\beta 4$ -targeting cells. Fifteen fields were analyzed from each of two independent experiments. Plotted is the mean percentage of area per field stained for nuclei \pm s.d. $n = 30$. Data were analyzed by one-way ANOVA and Dunnett’s multiple comparisons test; (B,C) the polarized expression of $\beta 4$ in endothelial cells was analyzed at 3, 24, and 48 h; (B) representative images of endothelial cells at 24 h immunostained for the $\beta 4$ integrin subunit (green) and CD31 (red). Scale bar = 100 μ m; (C) plotted is the mean difference in $\beta 4$ /CD31 fluorescence intensity between polar ends of endothelial cells or cell cords using a constant ROI (see top panel in C for diagram) \pm s.e.m. Fifteen fields were analyzed from three independent experiments ($n = 3$ independent experiments). Data were analyzed by one-way ANOVA and the Tukey’s multiple comparisons test. **** $p \leq 0.0001$.

The $\alpha 6\beta 4$ integrin is polarized to the leading edge of migrating epithelial cells to promote their migration [37–39]. The $\alpha 6\beta 4$ integrin has also been observed at the tips of sprouting vessels in vivo [40]. Thus, we were interested in examining the localization of $\alpha 6\beta 4$ during the formation of endothelial tubes. In these experiments, we employed a second organotypic assay, referred to as the planar co-culture assay. In this assay, endothelial cells are plated at low density on a confluent layer of dermal fibroblasts, which become embedded in a dense fibronectin matrix. Endothelial cells attach and spread within 1 h and begin to elongate, migrate and form cords after approximately 24 h [7,41]. Therefore, we employed immunofluorescence microscopy to examine the cellular localization of endothelial $\alpha 6\beta 4$ at 3, 24 and 48 h. Co-cultures were immunostained for the $\beta 4$ subunit and the endothelial marker, CD31 (Figure 3B). This was feasible as fibroblasts that are present in the co-culture do not express either $\alpha 6\beta 4$ or CD31. To measure the polarized distribution of $\alpha 6\beta 4$ in endothelial cells/cords, we used CD31 to establish the endothelial area and determined the difference in $\beta 4$ fluorescence intensity on either ends of endothelial cells or cords using a constant-sized ROI (Figure 3C, top panel). At 3 h of co-culture, individual endothelial cells are easily distinguishable. Little polarized localization was observed at this time (Figure 3C). At 24 and 48 h, when endothelial cords had begun to form cords [7,41], the localization of $\alpha 6\beta 4$ was predominately stronger at one end of the endothelial structure (Figure 3C). Although we cannot discern whether the concentrated localization occurs at the migrating front, the polarized distribution of $\alpha 6\beta 4$ is consistent with its role in endothelial migration and the localization of $\alpha 6\beta 4$ in sprouting vessels in vivo.

3.4. Integrin $\alpha 6\beta 4$ Promotes the Expression of ANGPT2 and Other Angiogenesis-Associated Genes

Since we determined that $\alpha 6\beta 4$ contributed to both cell migration and endothelial sprouting, we next sought to determine whether it also contributed to the regulation of the angiogenesis-associated genes that we previously identified to be inhibited in $\alpha 6$ -depleted cells. Expression of the $\alpha 5$ chain of laminin (LAMA5) of laminin-511, CXCR4, and ANGPT2 mRNA transcripts were previously determined to be positively associated

with the expression of endothelial $\alpha 6$ integrins [7]. To evaluate the contribution of $\alpha 6\beta 4$ to the expression of these genes, we isolated RNA from endothelial cells treated with non-targeting and $\beta 4$ -targeting siRNA from 6-day bead-sprout assays (shown in Figure 3) and analyzed gene expression by qPCR (Figure 4). The expression of $\beta 4$ mRNA was significantly reduced by all three $\beta 4$ -targeting siRNAs (Figure 4A). Interestingly, a significant decrease in ANGPT2 expression was also observed with all three $\beta 4$ -targeting siRNAs (Figure 4B), indicating that $\alpha 6\beta 4$ contributes to the regulation of ANGPT2 mRNA expression. The expression of LAMA5 was significantly decreased in cells treated with either of the two $\beta 4$ -targeting siRNAs (Figure 4C), while trending downward in cells treated with a third siRNA. These data suggest that $\alpha 6\beta 4$ promotes the expression of LAMA5 mRNA. Notably, the expression of CXCR4 was not inhibited in $\beta 4$ -depleted endothelial cells (Figure 4D), suggesting that $\alpha 6\beta 1$ is likely to be responsible for the previously described regulation of CXCR4 by $\alpha 6$ integrins [7]. Similar to our published results for $\alpha 6$ -depleted endothelial cells, the expression of the $\alpha 4$ chain (LAMA4) of laminin-411 was not affected in $\beta 4$ -depleted cells (Figure 4E).

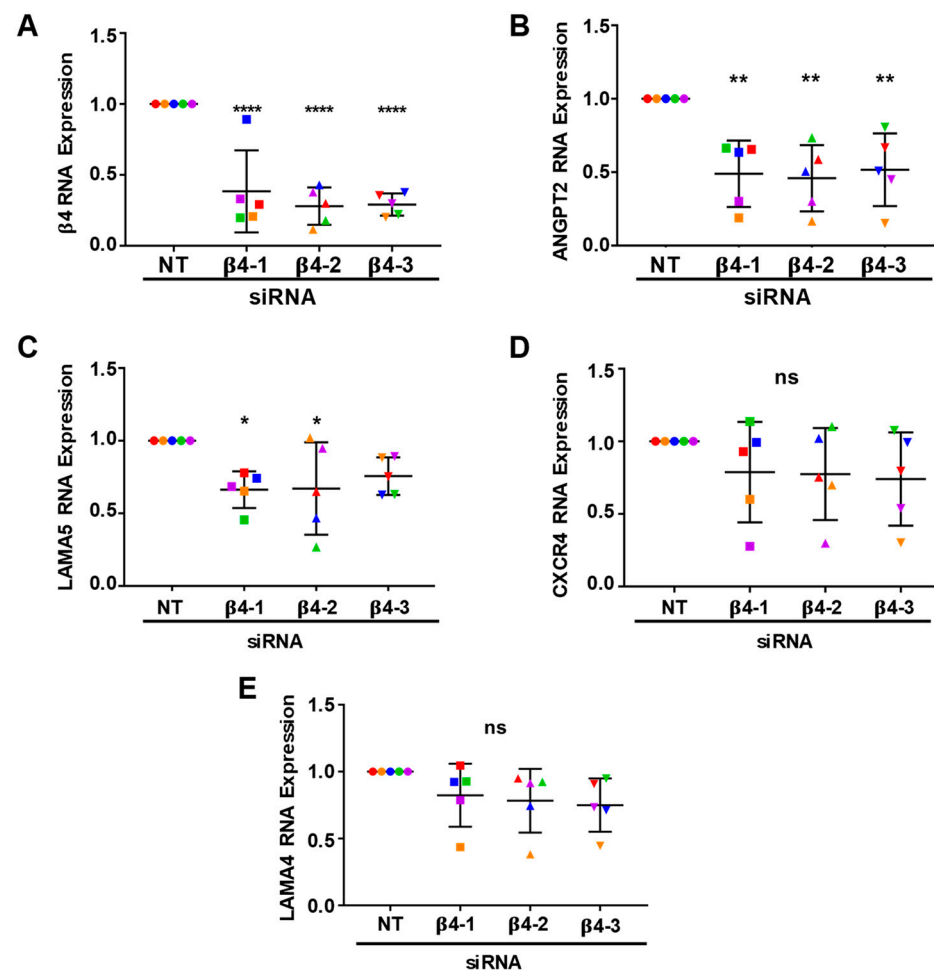


Figure 4. The expression ANGPT2 is positively regulated by integrin $\alpha 6\beta 4$. RNA was isolated from 6-day bead sprouts and analyzed by qPCR: (A) Shown is the efficiency of $\beta 4$ depletion using three distinct siRNA targeting sequences (also shown in Figure 2A) and the effects of $\beta 4$ depletion on the expression of the (B) ANGPT2, (C) LAMA5, (D) CXCR4, and (E) LAMA4. Data were normalized to β -actin and then to the non-targeting (NT) control. Plotted is the mean RNA expression \pm s.d. $n = 5$ independent experiments. Data were analyzed using a Single-Sample t -test. Each independent experiment is represented by a different color. ns = not significant, * $p \leq 0.05$, ** $p \leq 0.01$, *** $p \leq 0.0001$.

To determine whether the depletion of $\alpha 6\beta 4$ integrin affected the expression of other angiogenesis-associated genes [42–44], we analyzed the expression of Delta-like ligand 4 (DLL4), Jagged-1 (JAG1), Jagged-2 (JAG2), vascular endothelial growth factor receptor 2 (KDR), neuropilin-1 (NRP1), inhibitor of DNA-binding 1 (ID1), inhibitor of DNA-binding 2 (ID2), and Platelet-derived growth factor β (PDGFB) genes by qPCR (Figure 5A–C). The results indicate that the expression of NRP1 mRNA was significantly inhibited by all three $\beta 4$ -targeting siRNAs. Additionally, a significant downregulation of PDGFB mRNA was observed with two of the three $\beta 4$ -targeting siRNAs, with the third siRNA exhibiting a downward trend (Figure 5A,B). Taken together, these results suggest that $\alpha 6\beta 4$ contributes to positive regulation of the expression of ANGPT2 and NRP1 RNA transcripts, and it is likely to promote the expression of PDGFB and LAMA5 mRNAs as well.

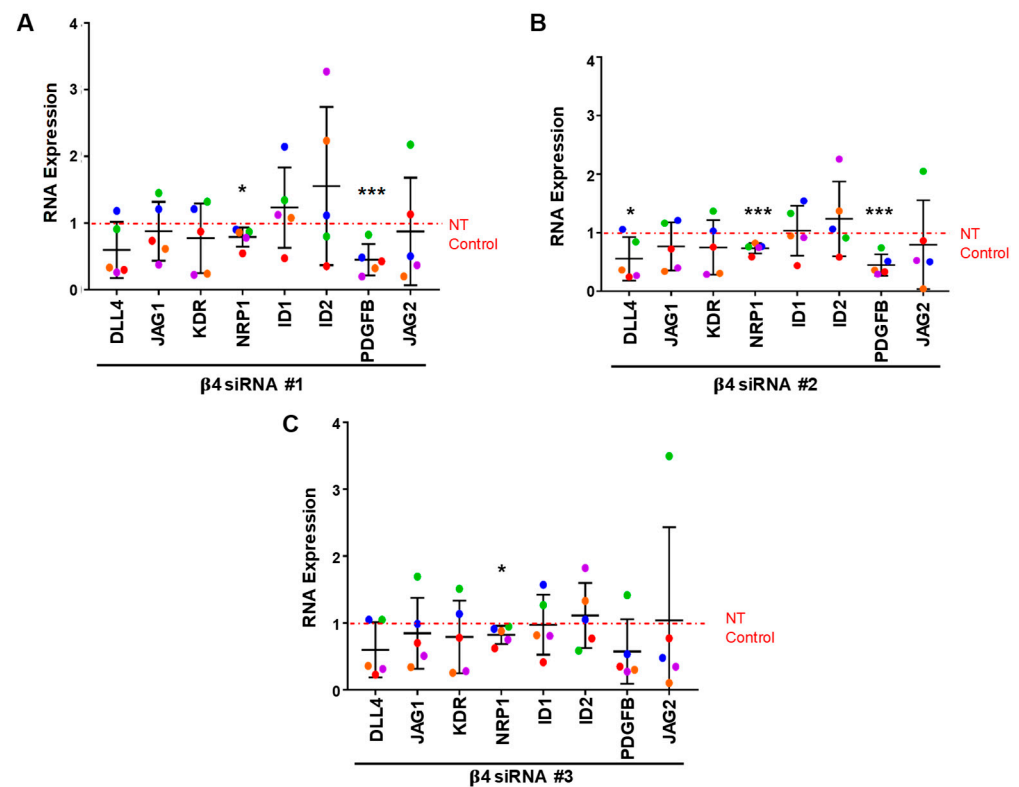


Figure 5. The expression of NRP1 and PDGFB are positively associated with integrin $\alpha 6\beta 4$ expression. Changes in RNA expression in 5-day bead-sprout assays of $\beta 4$ -depleted endothelial cells and control cells were measured by qPCR. The efficiency of $\beta 4$ depletion using 3 siRNA targeting sequences was previously shown in Figure 4. Effects of $\beta 4$ knockdown with siRNA #1 (A), siRNA #2 (B), or siRNA# 3 (C) on the expression of genes associated with angiogenesis. Data were normalized to β -actin and then to non-targeting (NT) control. Plotted is the mean RNA expression \pm s.d. $n = 5$ independent experiments. Mean expression of each gene was compared to non-targeting (NT) control. Data were analyzed using a Single-Sample t -test. Each independent experiment is represented by a different color. * $p \leq 0.05$, *** $p \leq 0.001$.

3.5. Integrin $\alpha 3\beta 1$ Plays Overlapping and Distinct Roles during Endothelial Morphogenesis

In addition to $\alpha 6\beta 1$ and $\alpha 6\beta 4$, endothelial cells also express integrin $\alpha 3\beta 1$ to engage their laminin substrates [10,45]. Since the expression of $\alpha 3\beta 1$ was found to be a negative regulator of angiogenesis in vivo [14], we questioned whether it served a similar role in our organotypic cultures. To determine whether the depletion of $\alpha 3\beta 1$ enhanced endothelial morphogenesis, we employed lentiviral vectors for the doxycycline inducible expression of either non-targeting (NT) or $\alpha 3$ -targeting shRNA that was accompanied by the expression of an RFP reporter. The induction of the expression of $\alpha 3$ -targeting shRNA significantly inhibited the expression of the $\alpha 3$ subunit, and thus, the $\alpha 3\beta 1$ integrin (Figure 6A). Notably,

no effects on proliferation or survival were observed in 2D culture, consistent with $\alpha 3$ -depleted endothelial cells in vivo [15]. The efficient depletion of the $\alpha 3$ subunit from endothelial cells inhibited their ability to form sprouts in bead-sprout assays (Figure 6B,C). Images of 6-day bead-sprout assays with endothelial cells expressing either NT or $\alpha 3$ -targeting shRNA, together with RFP, are shown in Figure 6B. The quantification of three independent experiments is shown in Figure 6C. It is noteworthy that sprouting was severely inhibited in $\alpha 3$ -depleted cells. However, unlike the depletion of $\alpha 6$ -integrins, depletion of $\alpha 3\beta 1$ did not impact cell migration across gelatin-coated transwells (Figure 6D).

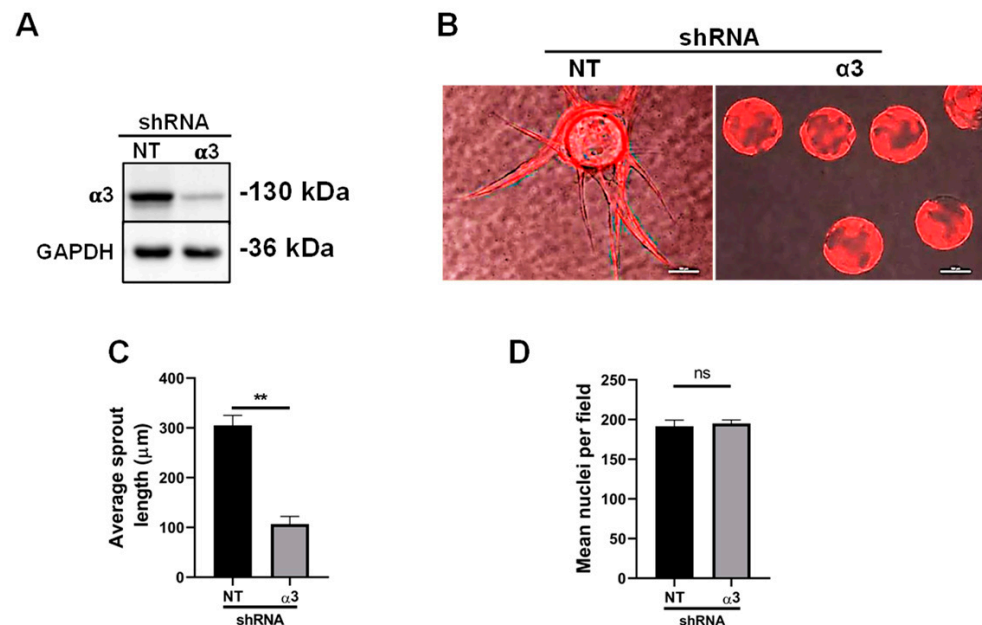


Figure 6. Depletion of endothelial integrin $\alpha 3\beta 1$ inhibits early endothelial morphogenesis but does not affect endothelial migration: (A) representative western blot of the expression of the $\alpha 3$ integrin subunit after induction of $\alpha 3$ -targeting or non-targeting (NT) shRNA; (B) representative images of 6-day bead-sprout assays. Shown are overlays of phase contrast and fluorescent images of the same fields of endothelial cells expressing RFP in conjunction with shRNA under doxycycline regulation. Scale bar = 100 μm ; (C) plotted is the mean sprout length measured from 3 independent experiments of 6-day bead-sprout assays with 10 randomly selected fields each, averaging 6–8 beads per field \pm s.e.m. $n = 3$ independent experiments; (D) analysis of nuclear staining in transwell migration assays with non-targeting (NT) or $\alpha 3$ -targeting cells. Five fields were analyzed from each of three independent experiments. Plotted is the mean area of nuclei per field, normalized to number of cells seeded \pm s.e.m. $n = 3$ independent experiments. Data were analyzed by two-tailed Student's *t*-test. ns = not significant, $** p \leq 0.01$.

3.6. Integrin $\alpha 3\beta 1$ Contributes to the Expression of a Distinct Set of Angiogenesis-Associated Genes

Since depletion of $\alpha 3\beta 1$ from endothelial cells also inhibited endothelial morphogenesis, we asked whether any of the genes that are regulated by $\alpha 6$ integrins ($\alpha 6\beta 1$ and/or $\alpha 6\beta 4$) are also regulated by $\alpha 3\beta 1$. For these gene expression studies, we depleted the $\alpha 3$ integrin subunit using siRNAs with three distinct targeting sequences. All three efficiently inhibited expression of the $\alpha 3$ subunit gene, as shown by qPCR analysis (Figure 7A). As a control, we asked whether depleting the cells of $\alpha 3\beta 1$ using siRNAs lead to defects in endothelial sprouting similar to the phenotype observed when $\alpha 3$ was depleted by shRNA. All three siRNAs resulted in a similar inhibition of endothelial morphogenesis (Figure 7B). Since our previous studies implicated $\alpha 6$ integrins in regulating the expression of LAMA5, ANGPT2, and CXCR4, but not LAMA4, we first examined the expression of these genes in $\alpha 3$ -depleted cells. RNA was harvested from $\alpha 3$ -depleted and control endothelial cells from 6-day bead-sprout assays and analyzed by qPCR. This analysis did not reveal significant

changes in LAMA4, LAMA5, ANGPT2 or CXCR4 expression (Figure 7C–F). Expanded qPCR analysis for other angiogenesis-associated genes identified a significant downregulation of NRP1 and ID1 with all three $\alpha 3$ -targeting siRNA sequences. A significant decrease in the expression of PDGFB mRNA was observed with two of the $\alpha 3$ -targeting sequences, with the third showing a downward trend (Figure 8A–C). These results suggest that $\alpha 3\beta 1$ regulates endothelial morphogenesis by distinct mechanisms, and that the loss of its expression cannot be compensated by $\alpha 6\beta 1$ or $\alpha 6\beta 4$. Notably, $\alpha 3\beta 1$ and $\alpha 6\beta 4$ regulated the expression of distinct but overlapping sets of angiogenesis-associated genes.

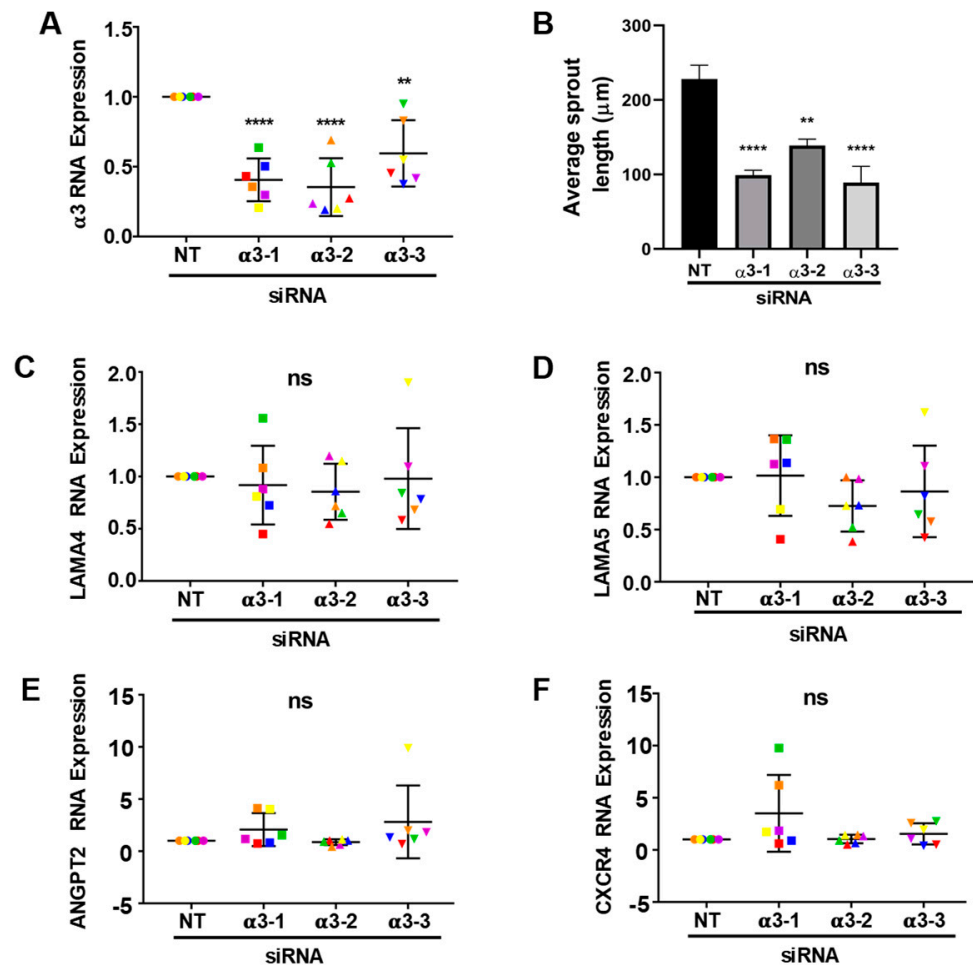


Figure 7. Integrin $\alpha 3\beta 1$ expression is not required for the expression of CXCR4, ANGPT2, LAMA4, and LAMA5. (A) The efficiency of $\alpha 3$ depletion using 3 siRNA-targeting sequences was determined by qPCR from 6 independent experiments. Data were normalized to β -actin and then to non-targeting (NT) control. Plotted is the mean RNA expression \pm s.d. $n = 6$ independent experiments. Data were analyzed by Single-Sample t -test; (B) quantitation of sprout length from 6–8 beads in each of 5 randomly selected fields in 6 independent experiments. Data plotted as the mean sprout length \pm s.e.m. $n = 6$ independent experiments. Data were analyzed by one-way ANOVA with Dunnett's multiple comparisons test; (C–F) the effects of $\alpha 3$ depletion on the expression of the LAMA5, LAMA4, ANGPT2, and CXCR4. Data were normalized to β -actin and then to non-targeting (NT) control. Plotted is the mean RNA expression \pm s.d. $n = 6$ independent experiments. Data were analyzed by Single-Sample t -test. Each independent experiment is represented by a distinct color. ns = not significant, ** $p \leq 0.01$, **** $p \leq 0.0001$.

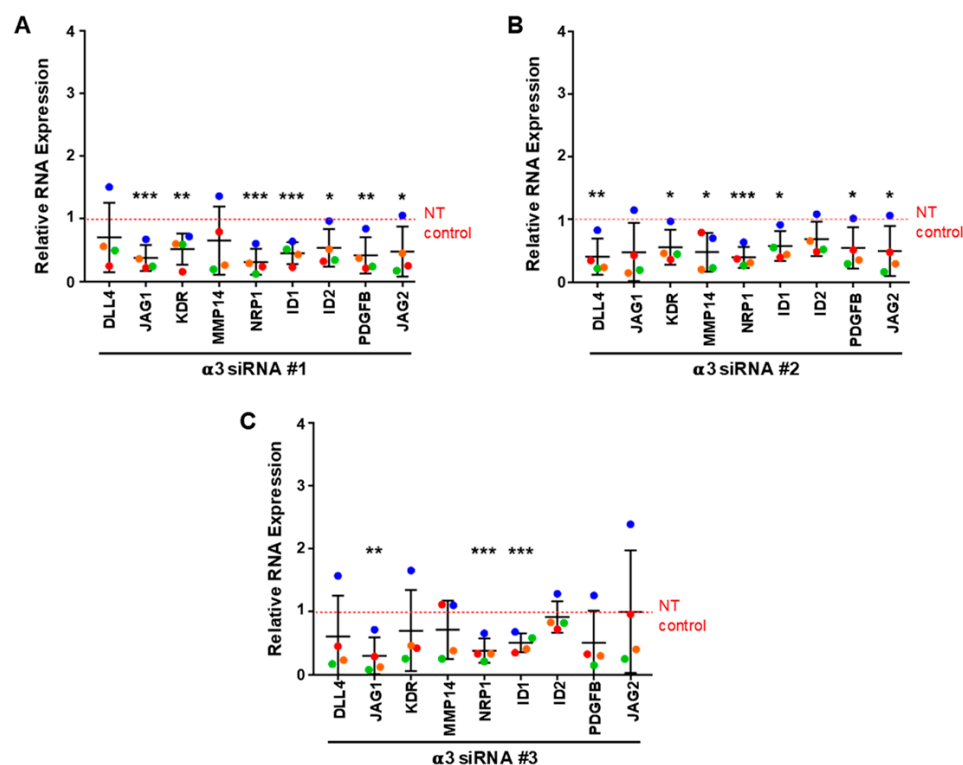


Figure 8. Regulation of angiogenesis-associated genes by integrin $\alpha 3\beta 1$. Changes in RNA expression in 5-day bead-sprout assays of $\alpha 3$ -depleted endothelial cells and control were measured by qPCR. The efficiency of $\alpha 3$ depletion using 3 siRNA targeting sequences previously shown in Figure 7. Effects of $\alpha 3$ knockdown with siRNA #1 (A), siRNA #2 (B), or siRNA# 3 (C) on the expression of genes associated with angiogenesis. Data were normalized to β -actin and then to non-targeting (NT) control. Plotted is the mean RNA expression \pm s.d. $n = 4$ independent experiments. Mean expression of each gene was compared to non-targeting (NT) control. Data were analyzed using a Single-Sample *t*-test. * $p \leq 0.05$, ** $p \leq 0.01$, *** $p \leq 0.001$.

4. Discussion

Taken together, our data suggest that endothelial laminin-binding integrins play overlapping and distinct roles during endothelial morphogenesis (Figure 9). Our previous studies indicated that the expression of integrin $\alpha 3\beta 1$ does not compensate for the depletion of $\alpha 6$ integrins in our assays [7]. Our current findings demonstrate that inhibiting the expression of $\alpha 3\beta 1$ also inhibits morphogenesis, indicating that $\alpha 6$ integrins do not compensate for the loss of $\alpha 3\beta 1$. Because the integrin $\beta 1$ subunit dimerizes with multiple α subunits, we were unable to directly identify specific roles for $\alpha 6\beta 1$. However, we did demonstrate that the $\alpha 6\beta 4$ integrin plays an essential role in promoting endothelial sprouting, suggesting that both $\alpha 6\beta 1$, and $\alpha 6\beta 4$ may contribute to these processes. Transcriptome analysis indicates that $\alpha 3\beta 1$, $\alpha 6\beta 1$, and $\alpha 6\beta 4$ regulate distinct sets of angiogenesis-associated genes at the level of mRNA expression (see Table S4). For example, our previous studies indicated that depletion of the $\alpha 6$ subunit inhibited the expression of both ANGPT2 and CXCR4; however, we did not determine whether $\alpha 6\beta 1$ and/or $\alpha 6\beta 4$ was responsible for this regulation [7]. Here, we show that depletion of $\alpha 6\beta 4$ resulted in the inhibition of the expression of ANGPT2 mRNA, but did not alter the expression of CXCR4. While the expression of $\alpha 6\beta 4$ is positively correlated with ANGPT2 mRNA expression, we are not excluding the possibility that $\alpha 6\beta 1$ may also contribute to ANGPT2 expression. Our data also indicate that $\alpha 6\beta 4$ does not significantly contribute the expression of CXCR4 mRNA; this suggests that $\alpha 6\beta 1$ is responsible for regulating the expression of CXCR4 and that $\alpha 6\beta 1$ regulates endothelial morphogenesis, at least in part without contribution from $\alpha 6\beta 4$, as the expression of recombinant CXCR4 partially rescued endothelial morphogenesis when

the $\alpha 6$ subunit was depleted [7]. Notably, the depletion of $\alpha 3\beta 1$ did not alter the expression of ANGPT2 or CXCR4, supporting its distinct role in endothelial cells.

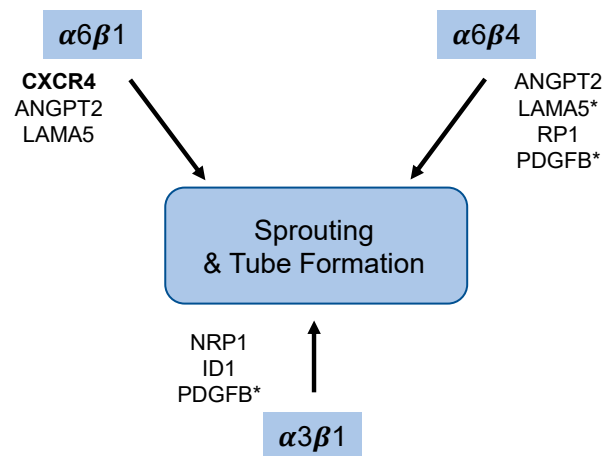


Figure 9. Schematic summary. RNAi-dependent depletion of the $\alpha 3\beta 1$ or the $\alpha 6$ integrins, $\alpha 6\beta 1$ and $\alpha 6\beta 4$ inhibits endothelial sprouting and tube formation in organotypic co-culture models. The expression of CXCR4 shown in bold was inhibited only by the depletion of the integrin $\alpha 6$ subunit, and not by depletion of either the $\beta 4$ or $\alpha 3$ subunit, suggesting that $\alpha 6\beta 1$ is the only laminin-binding integrin that impacts CXCR4 expression (Figures 4 and 7 and [7]). Depletion of either the $\alpha 6$ or $\beta 4$ subunit inhibited migration, as well as the expression of ANGPT2 and LAMA5 mRNA; this suggests that $\alpha 6\beta 4$ regulates the expression of these genes, but does not exclude the possibility of a contribution from $\alpha 6\beta 1$. The depletion of $\alpha 3\beta 1$ or $\alpha 6\beta 4$ inhibited the expression of NRP1 and PDGFB, whereas the expression of ID1 was only inhibited by the depletion of $\alpha 3\beta 1$. * Indicate genes whose expression was significantly inhibited by two of the three siRNA-targeting sequences.

Others have shown that the overexpression of the $\alpha 6$ and $\beta 4$ subunits in cultured endothelial cells promotes transwell migration on a laminin-332 substrate [22]. We demonstrated that endogenously expressed $\alpha 6\beta 4$ positively regulates migration in cultured endothelial cells without the addition of a laminin substrate or the need for overexpression. Interestingly, our published studies demonstrated that the endothelial expression of laminin-511, a ligand for $\alpha 6\beta 4$, is regulated by $\alpha 6$ integrins [7] (Figure 4C). Thus, $\alpha 6$ -dependent regulation of laminin-511 may be involved in promoting migration by $\alpha 6\beta 4$ as observed in our current studies (Figure 2C) and explain why $\alpha 3\beta 1$ is not required for migration in our assays (Figures 6D and 7D). It is important to note that others have demonstrated, in other cell types, that $\alpha 6\beta 4$ can promote migration on non-laminin substrates, suggesting the possibility that $\alpha 6\beta 4$ may regulate cell migration by a ligand-independent mechanism [46].

In epithelial cells, $\alpha 6\beta 4$ becomes polarized at the leading edge of migrating epithelial cells to promote their migration [37–39]. We demonstrated that endothelial $\alpha 6\beta 4$ also contributes to endothelial cell migration. We observed the polarized localization of $\alpha 6\beta 4$ during the migratory phase of endothelial tube morphogenesis in planar co-culture, similar to the polarized endothelial expression of $\alpha 6\beta 4$ at the tips of endothelial sprouts during neovascularization in human neonatal foreskins [40]. We had previously demonstrated that $\alpha 6\beta 4$ associates with the vimentin intermediate filament by mechanisms that require the $\beta 4$ subunit cytoplasmic domain [47,48]. Interestingly, recent studies demonstrated that $\alpha 6\beta 4$ localizes with vimentin in puncta in lamellipodia at the leading edge, to promote the migration of epithelial cells [49]. Thus, the $\alpha 6\beta 4$ integrin may similarly regulate migration in endothelial cells.

Sprouting angiogenesis requires the invasion of endothelial cells into the surrounding ECM [50]. The inhibition of sprouting by $\beta 4$ -depleted endothelial cells in our bead-sprout assays suggests that $\alpha 6\beta 4$ may also promote invasion during angiogenesis. Notably, $\alpha 6\beta 4$ has been shown to contribute to cancer cell invasion [37], indicating that the $\alpha 6\beta 4$ integrin likely contributes to invasion in multiple cellular contexts. Importantly, others have

identified a role for endothelial $\alpha\beta 1$ integrins both in culture and in vivo in the formation of invasive structures known as podosome rosettes, which concentrate the membrane-associated protease, MT1-MMP [19]. The $\alpha\beta 1$, but not the $\alpha\beta 4$ integrin, was recruited to rosettes, at least when its localization was examined in cell culture [19], suggesting that $\alpha\beta 1$ and $\alpha\beta 4$ likely contribute to invasion by different mechanisms. It will be important to identify the mechanisms by which $\alpha\beta 4$ contributes to endothelial invasion and how these differ from $\alpha\beta 1$.

Our current study identified a role for $\alpha\beta 4$ in the regulation of ANGPT2 mRNA, although we cannot exclude the possibility that $\alpha\beta 1$ also contributes to this regulation. Angiopoietin-2 (product of the ANGPT2 gene) serves as an antagonist to Tie-signaling activated by angiopoietin-1 [42,50,51]. Since angiopoietin-1 is secreted by neighboring mural cells in vivo, it is unclear how the loss of angiopoietin-2 expression in our organotypic model inhibits morphogenesis. However, some studies have indicated that angiopoietin-2 can activate Tie-2 in an autocrine fashion, suggesting that angiopoietin-2 may have a cell-autonomous effect in promoting new vessel formation [52]. This possibility would be interesting to address in future studies.

Additionally, our results indicate that $\alpha 6$ integrins do not compensate for the loss of $\alpha 3\beta 1$, as depletion of the $\alpha 3$ subunit also inhibited morphogenesis in bead-sprout assays, suggesting that $\alpha 3\beta 1$ regulates these processes by distinct mechanisms. Consistent with this notion, the loss of $\alpha 3\beta 1$ expression did not inhibit migration in our assays and affected the expression of a distinct set of angiogenesis-associated genes compared to those regulated by $\alpha 6$ integrins (Table S4). In vivo studies by da Silva and colleagues reported that endothelial $\alpha 3\beta 1$ acted as a repressor of pathological angiogenesis, as its deletion enhanced tumor-associated angiogenesis through the upregulation of KDR (VEGFR2) [15]. We did not observe an upregulation of KDR/VEGFR2, at least at the transcript level; however, we did not test whether the translation of VEGFR2 was altered in our assay. It is important to note that although da Silva and colleagues demonstrated that the expression of $\alpha 3\beta 1$ was absent from tumor-associated vessels, blood vessels in the surrounding normal skin were still positive for $\alpha 3\beta 1$ [15]. This implies that endothelial $\alpha 3\beta 1$ was present during the initiation of tumor-induced angiogenesis. Thus, this in vivo model may not be ideal to examine the role of $\alpha 3\beta 1$ during the initial steps of angiogenesis, when endothelial cells first respond to angiogenic signals, and may explain the differences with our current findings.

Interestingly, we observed the downregulation of NRP1 and ID1 using all three $\alpha 3$ siRNA-targeting sequences. NRP1 is a critical protein enriched with tip cells; it functions as a co-receptor for VEGFR2 signaling [53], and contributes to angiogenesis, in part by promoting the formation of filopodia through the activation of CDC42 [54]. It will be interesting to determine whether the expression of recombinant NRP1 can rescue the defects in morphogenesis in cells depleted of $\alpha 3\beta 1$. It is important to note that we also observed a downregulation of NRP1 expression using all three siRNAs targeting the $\beta 4$ subunit, suggesting that $\alpha\beta 4$ also contributes to the regulation of NRP1 expression. We did not observe the inhibition of NRP1 expression in $\alpha 6$ -depleted cells, presumably because $\alpha\beta 4$ is more efficiently depleted when siRNA targeting the $\beta 4$ subunit is employed.

As indicated above, $\alpha 3\beta 1$ promotes the expression of ID1, a transcriptional regulator, which plays a role in angiogenesis during embryogenesis and tumor formation, as well as during endothelial morphogenesis in cell culture models [55–59]. Further studies are needed to determine whether the downregulation of ID1 contributes to the observed phenotype in $\alpha 3$ -depleted endothelial cells in our organotypic assays. It is important to note that the $\alpha 3\beta 1$ integrin likely promotes angiogenesis by multiple mechanisms. For example, in endothelial cells, $\alpha 3\beta 1$ forms a ternary complex with the tetraspanin CD151 and the membrane-anchored matrix metalloproteinase and MT1-MMP, to promote appropriate proteolysis; the loss of CD151 results in a dramatic loss of $\alpha 3\beta 1$ /MT1-MMP association [60]. These observations have significant implications, as CD151 has been shown to promote angiogenesis [61]. Interestingly, $\alpha 3\beta 1$ has been associated with tumor-cell invasion [62] and has been shown to regulate MMP-9 RNA stability in keratinocytes [63,64]. Given the

matrix-dense environment of organotypic assays employed in our studies, the positive regulation of proteases by endothelial $\alpha 3\beta 1$ during morphogenesis could possibly explain the lack of tube formation and sprouting by $\alpha 3$ -depleted endothelial cells.

In summary, our current studies demonstrate that the expression of $\alpha 6\beta 4$ and $\alpha 3\beta 1$ regulate endothelial sprouting in our organotypic angiogenesis assay by non-redundant mechanisms, and regulate the expression of distinct sets of angiogenesis-associated genes. It will be important to identify the molecular mechanisms involved. Future studies are needed to determine the signaling pathways downstream of integrins that regulate the expression of these genes, and how these genes functionally contribute to processes needed for angiogenesis.

Supplementary Materials: The following are available online at <https://www.mdpi.com/article/10.3390/cells11050816/s1>, Figure S1: Integrin $\alpha 6\beta 4$ is primarily expressed in the arterial vessels of adult mouse retina; Figure S2: Integrin $\alpha 6\beta 4$ is expressed on the surface of HUVECs; Table S1: Antibodies; Table S2: RNAi; Table S3: QPCR Primers; Table S4: Summary of Gene Expression Analysis.

Author Contributions: Conceptualization, H.X. and S.E.L.; methodology, H.X.; validation, H.X.; investigation, H.X.; resources, S.E.L.; writing—original draft preparation, H.X.; writing—review and editing, H.X. and S.E.L.; supervision, S.E.L.; project administration, S.E.L.; funding acquisition, S.E.L. All authors have read and agreed to the published version of the manuscript.

Funding: This research received no external funding and was supported by the seed funds provided by Albany Medical College.

Institutional Review Board Statement: All animal experiments and procedures were performed in accordance with the Albany Medical College Institutional Animal Care and Use Committee (IACUC) regulations. Experiments were carried out in accordance with protocols 18-05003 and 18-07001 approved by the Albany Medical College IACUC.

Informed Consent Statement: Not applicable.

Data Availability Statement: This study did not report any datasets to be publicly archived.

Acknowledgments: The authors thank the Imaging Core of Albany Medical College for assistance in the preparation of immunofluorescence images, C. Michael DiPersio for critical reading of the manuscript, and Deborah Moran for assistance in the preparation of the manuscript.

Conflicts of Interest: The authors declare no conflict of interest.

References

1. Carmeliet, P. Angiogenesis in health and disease. *Nat. Med.* **2003**, *9*, 653–660. [[CrossRef](#)] [[PubMed](#)]
2. Carmeliet, P. Angiogenesis in life, disease and medicine. *Nature* **2005**, *438*, 932–936. [[CrossRef](#)]
3. Senger, D.R.; Davis, G.E. Angiogenesis. *Cold Spring Harb. Perspect. Biol.* **2011**, *3*, a005090. [[CrossRef](#)] [[PubMed](#)]
4. Eming, S.A.; Brachvogel, B.; Odorisio, T.; Koch, M. Regulation of angiogenesis: Wound healing as a model. *Prog. Histochem. Cytochem.* **2007**, *42*, 115–170. [[CrossRef](#)]
5. Hallmann, R.; Horn, N.; Selg, M.; Wendler, O.; Pausch, F.; Sorokin, L.M. Expression and function of laminins in the embryonic and mature vasculature. *Physiol. Rev.* **2005**, *85*, 979–1000. [[CrossRef](#)]
6. Turner, C.J.; Badu-Nkansah, K.; Hynes, R.O. Endothelium-derived fibronectin regulates neonatal vascular morphogenesis in an autocrine fashion. *Angiogenesis* **2017**, *20*, 519–531. [[CrossRef](#)] [[PubMed](#)]
7. Xu, H.; Pumiglia, K.; LaFlamme, S.E. Laminin-511 and alpha6 integrins regulate the expression of CXCR4 to promote endothelial morphogenesis. *J. Cell Sci.* **2020**, *133*, jcs246595. [[CrossRef](#)]
8. Song, J.; Zhang, X.; Buscher, K.; Wang, Y.; Wang, H.; Di Russo, J.; Li, L.; Lutke-Enking, S.; Zarbock, A.; Stadtmann, A.; et al. Endothelial Basement Membrane Laminin 511 Contributes to Endothelial Junctional Tightness and Thereby Inhibits Leukocyte Transmigration. *Cell Rep.* **2017**, *18*, 1256–1269. [[CrossRef](#)]
9. Avraamides, C.J.; Garmy-Susini, B.; Varner, J.A. Integrins in angiogenesis and lymphangiogenesis. *Nat. Rev. Cancer* **2008**, *8*, 604–617. [[CrossRef](#)]
10. Nishiuchi, R.; Takagi, J.; Hayashi, M.; Ido, H.; Yagi, Y.; Sanzen, N.; Tsuji, T.; Yamada, M.; Sekiguchi, K. Ligand-binding specificities of laminin-binding integrins: A comprehensive survey of laminin-integrin interactions using recombinant alpha3beta1, alpha6beta1, alpha7beta1 and alpha6beta4 integrins. *Matrix. Biol.* **2006**, *25*, 189–197. [[CrossRef](#)]

11. Kikkawa, Y.; Yu, H.; Genersch, E.; Sanzen, N.; Sekiguchi, K.; Fassler, R.; Campbell, K.P.; Talts, J.F.; Ekblom, P. Laminin isoforms differentially regulate adhesion, spreading, proliferation, and ERK activation of beta1 integrin-null cells. *Exp. Cell Res.* **2004**, *300*, 94–108. [[CrossRef](#)] [[PubMed](#)]
12. Kreidberg, J.A.; Donovan, M.J.; Goldstein, S.L.; Rennke, H.; Shepherd, K.; Jones, R.C.; Jaenisch, R. Alpha 3 beta 1 integrin has a crucial role in kidney and lung organogenesis. *Development* **1996**, *122*, 3537–3547. [[CrossRef](#)] [[PubMed](#)]
13. Georges-Labouesse, E.; Messaddeq, N.; Yehia, G.; Cadalbert, L.; Dierich, A.; Le Meur, M. Absence of integrin alpha 6 leads to epidermolysis bullosa and neonatal death in mice. *Nat. Genet.* **1996**, *13*, 370–373. [[CrossRef](#)] [[PubMed](#)]
14. Dowling, J.; Yu, Q.C.; Fuchs, E. Beta4 integrin is required for hemidesmosome formation, cell adhesion and cell survival. *J. Cell Biol.* **1996**, *134*, 559–572. [[CrossRef](#)] [[PubMed](#)]
15. da Silva, R.G.; Tavora, B.; Robinson, S.D.; Reynolds, L.E.; Szekeres, C.; Lamar, J.; Batista, S.; Kostourou, V.; Germain, M.A.; Reynolds, A.R.; et al. Endothelial alpha3beta1-integrin represses pathological angiogenesis and sustains endothelial-VEGF. *Am. J. Pathol.* **2010**, *177*, 1534–1548. [[CrossRef](#)]
16. Germain, M.; De Arcangelis, A.; Robinson, S.D.; Baker, M.; Tavora, B.; D’Amico, G.; Silva, R.; Kostourou, V.; Reynolds, L.E.; Watson, A.; et al. Genetic ablation of the alpha 6-integrin subunit in Tie1Cre mice enhances tumour angiogenesis. *J. Pathol.* **2010**, *220*, 370–381. [[CrossRef](#)]
17. Bouvard, C.; De Arcangelis, A.; Dizier, B.; Galy-Fauroux, I.; Fischer, A.M.; Georges-Labouesse, E.; Helley, D. Tie2-dependent knockout of alpha6 integrin subunit in mice reduces post-ischaemic angiogenesis. *Cardiovasc. Res.* **2012**, *95*, 39–47. [[CrossRef](#)]
18. Bouvard, C.; Segaula, Z.; De Arcangelis, A.; Galy-Fauroux, I.; Mauge, L.; Fischer, A.M.; Georges-Labouesse, E.; Helley, D. Tie2-dependent deletion of alpha6 integrin subunit in mice reduces tumor growth and angiogenesis. *Int. J. Oncol.* **2014**, *45*, 2058–2064. [[CrossRef](#)]
19. Seano, G.; Chiaverina, G.; Gagliardi, P.A.; di Blasio, L.; Puliafito, A.; Bouvard, C.; Sessa, R.; Tarone, G.; Sorokin, L.; Helley, D.; et al. Endothelial podosome rosettes regulate vascular branching in tumour angiogenesis. *Nat. Cell Biol.* **2014**, *16*, 931–941. [[CrossRef](#)]
20. Welser-Alves, J.V.; Boroujerdi, A.; Tigges, U.; Wrabetz, L.; Feltri, M.L.; Milner, R. Endothelial beta4 integrin is predominantly expressed in arterioles, where it promotes vascular remodeling in the hypoxic brain. *Arterioscler. Thromb. Vasc. Biol.* **2013**, *33*, 943–953. [[CrossRef](#)]
21. Welser, J.V.; Halder, S.K.; Kant, R.; Boroujerdi, A.; Milner, R. Endothelial alpha6beta4 integrin protects during experimental autoimmune encephalomyelitis-induced neuroinflammation by maintaining vascular integrity and tight junction protein expression. *J. Neuroinflammation* **2017**, *14*, 217. [[CrossRef](#)]
22. Nikolopoulos, S.N.; Blaikie, P.; Yoshioka, T.; Guo, W.; Giancotti, F.G. Integrin beta4 signaling promotes tumor angiogenesis. *Cancer Cell* **2004**, *6*, 471–483. [[CrossRef](#)] [[PubMed](#)]
23. Desai, D.; Singh, P.; Van De Water, L.; Laflamme, S.E. Dynamic Regulation of Integrin alpha6beta4 During Angiogenesis: Potential Implications for Pathogenic Wound Healing. *Adv. Wound Care* **2013**, *2*, 401–409. [[CrossRef](#)] [[PubMed](#)]
24. Bishop, E.T.; Bell, G.T.; Bloor, S.; Broom, I.J.; Hendry, N.F.; Wheatley, D.N. An in vitro model of angiogenesis: Basic features. *Angiogenesis* **1999**, *3*, 335–344. [[CrossRef](#)] [[PubMed](#)]
25. Bajaj, A.; Li, Q.F.; Zheng, Q.; Pumiglia, K. Loss of NF1 expression in human endothelial cells promotes autonomous proliferation and altered vascular morphogenesis. *PLoS ONE* **2012**, *7*, e49222. [[CrossRef](#)]
26. Nakatsu, M.N.; Hughes, C.C. An optimized three-dimensional in vitro model for the analysis of angiogenesis. *Methods Enzymol.* **2008**, *443*, 65–82.
27. Varney, S.D.; Betts, C.B.; Zheng, R.; Wu, L.; Hinz, B.; Zhou, J.; Van De Water, L. Hic-5 is required for myofibroblast differentiation by regulating mechanically dependent MRTF-A nuclear accumulation. *J. Cell Sci.* **2016**, *129*, 774–787. [[CrossRef](#)]
28. Zheng, R.; Longmate, W.M.; DeFreest, L.; Varney, S.; Wu, L.; DiPersio, C.M.; Van De Water, L. Keratinocyte Integrin alpha3beta1 Promotes Secretion of IL-1alpha to Effect Paracrine Regulation of Fibroblast Gene Expression and Differentiation. *J. Investig. Dermatol.* **2019**, *139*, 2029–2038.e3. [[CrossRef](#)]
29. He, L.; Vanlandewijck, M.; Mae, M.A.; Andrae, J.; Ando, K.; Del Gaudio, F.; Nahar, K.; Lebouvier, T.; Lavina, B.; Gouveia, L.; et al. Single-cell RNA sequencing of mouse brain and lung vascular and vessel-associated cell types. *Sci. Data* **2018**, *5*, 180160. [[CrossRef](#)]
30. Sonnenberg, A.; Linders, C.J.; Daams, J.H.; Kennel, S.J. The alpha 6 beta 1 (VLA-6) and alpha 6 beta 4 protein complexes: Tissue distribution and biochemical properties. *J. Cell Sci.* **1990**, *96 Pt 2*, 207–217. [[CrossRef](#)]
31. Hiran, T.S.; Mazurkiewicz, J.E.; Kreienberg, P.; Rice, F.L.; LaFlamme, S.E. Endothelial expression of the alpha6beta4 integrin is negatively regulated during angiogenesis. *J. Cell Sci.* **2003**, *116*, 3771–3781. [[CrossRef](#)] [[PubMed](#)]
32. Nakatsu, M.N.; Sainson, R.C.; Aoto, J.N.; Taylor, K.L.; Aitkenhead, M.; Perez-del-Pulgar, S.; Carpenter, P.M.; Hughes, C.C. Angiogenic sprouting and capillary lumen formation modeled by human umbilical vein endothelial cells (HUVEC) in fibrin gels: The role of fibroblasts and Angiopoietin-1. *Microvasc. Res.* **2003**, *66*, 102–112. [[CrossRef](#)]
33. Newman, A.C.; Nakatsu, M.N.; Chou, W.; Gershon, P.D.; Hughes, C.C. The requirement for fibroblasts in angiogenesis: Fibroblast-derived matrix proteins are essential for endothelial cell lumen formation. *Mol. Biol. Cell* **2011**, *22*, 3791–3800. [[CrossRef](#)] [[PubMed](#)]
34. Nguyen, B.P.; Ryan, M.C.; Gil, S.G.; Carter, W.G. Deposition of laminin 5 in epidermal wounds regulates integrin signaling and adhesion. *Curr. Opin. Cell Biol.* **2000**, *12*, 554–562. [[CrossRef](#)]

35. Frank, D.E.; Carter, W.G. Laminin 5 deposition regulates keratinocyte polarization and persistent migration. *J. Cell Sci.* **2004**, *117*, 1351–1363. [[CrossRef](#)]
36. Hamelers, I.H.; Olivo, C.; Mertens, A.E.; Pegtel, D.M.; van der Kammen, R.A.; Sonnenberg, A.; Collard, J.G. The Rac activator Tiam1 is required for (alpha)3(beta)1-mediated laminin-5 deposition, cell spreading, and cell migration. *J. Cell Biol.* **2005**, *171*, 871–881. [[CrossRef](#)]
37. Mercurio, A.M.; Rabinovitz, I.; Shaw, L.M. The alpha 6 beta 4 integrin and epithelial cell migration. *Curr. Opin. Cell Biol.* **2001**, *13*, 541–545. [[CrossRef](#)]
38. Colburn, Z.T.; Jones, J.C. alpha6beta4 Integrin Regulates the Collective Migration of Epithelial Cells. *Am. J. Respir. Cell Mol. Biol.* **2017**, *56*, 443–452. [[CrossRef](#)]
39. Elaimy, A.L.; Wang, M.; Sheel, A.; Brown, C.W.; Walker, M.R.; Amante, J.J.; Xue, W.; Chan, A.; Baer, C.E.; Goel, H.L.; et al. Real-time imaging of integrin beta4 dynamics using a reporter cell line generated by Crispr/Cas9 genome editing. *J. Cell Sci.* **2019**, *132*, jcs231241. [[CrossRef](#)]
40. Enenstein, J.; Kramer, R.H. Confocal microscopic analysis of integrin expression on the microvasculature and its sprouts in the neonatal foreskin. *J. Invest. Dermatol.* **1994**, *103*, 381–386. [[CrossRef](#)]
41. Mavria, G.; Vercoulen, Y.; Yeo, M.; Paterson, H.; Karasarides, M.; Marais, R.; Bird, D.; Marshall, C.J. ERK-MAPK signaling opposes Rho-kinase to promote endothelial cell survival and sprouting during angiogenesis. *Cancer Cell* **2006**, *9*, 33–44. [[CrossRef](#)] [[PubMed](#)]
42. del Toro, R.; Prahst, C.; Mathivet, T.; Siegfried, G.; Kaminker, J.S.; Larrivee, B.; Breant, C.; Duarte, A.; Takakura, N.; Fukamizu, A.; et al. Identification and functional analysis of endothelial tip cell-enriched genes. *Blood* **2010**, *116*, 4025–4033. [[CrossRef](#)] [[PubMed](#)]
43. Strasser, G.A.; Kaminker, J.S.; Tessier-Lavigne, M. Microarray analysis of retinal endothelial tip cells identifies CXCR4 as a mediator of tip cell morphology and branching. *Blood* **2010**, *115*, 5102–5110. [[CrossRef](#)] [[PubMed](#)]
44. De Smet, F.; Segura, I.; De Bock, K.; Hohensinner, P.J.; Carmeliet, P. Mechanisms of vessel branching: Filopodia on endothelial tip cells lead the way. *Arterioscler. Thromb. Vasc. Biol.* **2009**, *29*, 639–649. [[CrossRef](#)] [[PubMed](#)]
45. Stenzel, D.; Franco, C.A.; Estrach, S.; Mettouchi, A.; Sauvaget, D.; Rosewell, I.; Schertel, A.; Armer, H.; Domogatskaya, A.; Rodin, S.; et al. Endothelial basement membrane limits tip cell formation by inducing Dll4/Notch signalling in vivo. *EMBO Rep.* **2011**, *12*, 1135–1143. [[CrossRef](#)]
46. O'Connor, K.L.; Shaw, L.M.; Mercurio, A.M. Release of cAMP gating by the alpha6beta4 integrin stimulates lamellae formation and the chemotactic migration of invasive carcinoma cells. *J. Cell Biol.* **1998**, *143*, 1749–1760. [[CrossRef](#)]
47. Homan, S.M.; Mercurio, A.M.; LaFlamme, S.E. Endothelial cells assemble two distinct alpha6beta4-containing vimentin-associated structures: Roles for ligand binding and the beta4 cytoplasmic tail. *J. Cell Sci.* **1998**, *111 Pt 18*, 2717–2728. [[CrossRef](#)]
48. Homan, S.M.; Martinez, R.; Benware, A.; LaFlamme, S.E. Regulation of the association of alpha 6 beta 4 with vimentin intermediate filaments in endothelial cells. *Exp. Cell Res.* **2002**, *281*, 107–114. [[CrossRef](#)]
49. Colburn, Z.T.; Jones, J.C.R. Complexes of alpha6beta4 integrin and vimentin act as signaling hubs to regulate epithelial cell migration. *J. Cell Sci.* **2018**, *131*, jcs214593. [[CrossRef](#)]
50. Carmeliet, P.; Jain, R.K. Molecular mechanisms and clinical applications of angiogenesis. *Nature* **2011**, *473*, 298–307. [[CrossRef](#)]
51. Huang, H.; Bhat, A.; Woodnutt, G.; Lappe, R. Targeting the ANGPT-TIE2 pathway in malignancy. *Nat. Rev. Cancer* **2010**, *10*, 575–585. [[CrossRef](#)] [[PubMed](#)]
52. Thurston, G.; Daly, C. The complex role of angiopoietin-2 in the angiopoietin-tie signaling pathway. *Cold Spring Harb. Perspect. Med.* **2012**, *2*, a006550. [[CrossRef](#)] [[PubMed](#)]
53. Kofler, N.M.; Simons, M. Angiogenesis versus arteriogenesis: Neuropilin 1 modulation of VEGF signaling. *F1000Prime Rep.* **2015**, *7*, 26. [[CrossRef](#)] [[PubMed](#)]
54. Fantin, A.; Lampropoulou, A.; Gestri, G.; Raimondi, C.; Senatore, V.; Zachary, I.; Ruhrberg, C. NRP1 Regulates CDC42 Activation to Promote Filopodia Formation in Endothelial Tip Cells. *Cell Rep.* **2015**, *11*, 1577–1590. [[CrossRef](#)] [[PubMed](#)]
55. Benezra, R. Role of Id proteins in embryonic and tumor angiogenesis. *Trends Cardiovasc. Med.* **2001**, *11*, 237–241. [[CrossRef](#)]
56. Benezra, R.; Rafii, S.; Lyden, D. The Id proteins and angiogenesis. *Oncogene* **2001**, *20*, 8334–8341. [[CrossRef](#)]
57. Volpert, O.V.; Pili, R.; Sikder, H.A.; Nelius, T.; Zaichuk, T.; Morris, C.; Shiflett, C.B.; Devlin, M.K.; Conant, K.; Alani, R.M. Id1 regulates angiogenesis through transcriptional repression of thrombospondin-1. *Cancer Cell* **2002**, *2*, 473–483. [[CrossRef](#)]
58. Nishiyama, K.; Takaji, K.; Kataoka, K.; Kurihara, Y.; Yoshimura, M.; Kato, A.; Ogawa, H.; Kurihara, H. Id1 gene transfer confers angiogenic property on fully differentiated endothelial cells and contributes to therapeutic angiogenesis. *Circulation* **2005**, *112*, 2840–2850. [[CrossRef](#)]
59. Tanaka, A.; Itoh, F.; Nishiyama, K.; Takezawa, T.; Kurihara, H.; Itoh, S.; Kato, M. Inhibition of endothelial cell activation by bHLH protein E2-2 and its impairment of angiogenesis. *Blood* **2010**, *115*, 4138–4147. [[CrossRef](#)]
60. Yanez-Mo, M.; Barreiro, O.; Gonzalo, P.; Batista, A.; Megias, D.; Genis, L.; Sachs, N.; Sala-Valdes, M.; Alonso, M.A.; Montoya, M.C.; et al. MT1-MMP collagenolytic activity is regulated through association with tetraspanin CD151 in primary endothelial cells. *Blood* **2008**, *112*, 3217–3226. [[CrossRef](#)]
61. Sadej, R.; Grudowska, A.; Turczyk, L.; Kordek, R.; Romanska, H.M. CD151 in cancer progression and metastasis: A complex scenario. *Lab. Invest.* **2014**, *94*, 41–51. [[CrossRef](#)] [[PubMed](#)]

62. Mitchell, K.; Svenson, K.B.; Longmate, W.M.; Gkirtzimanaki, K.; Sadej, R.; Wang, X.; Zhao, J.; Eliopoulos, A.G.; Berditchevski, F.; DiPersio, C.M. Suppression of integrin alpha3beta1 in breast cancer cells reduces cyclooxygenase-2 gene expression and inhibits tumorigenesis, invasion, and cross-talk to endothelial cells. *Cancer Res.* **2010**, *70*, 6359–6367. [[CrossRef](#)] [[PubMed](#)]
63. DiPersio, C.M.; Shao, M.; Di Costanzo, L.; Kreidberg, J.A.; Hynes, R.O. Mouse keratinocytes immortalized with large T antigen acquire alpha3beta1 integrin-dependent secretion of MMP-9/gelatinase B. *J. Cell Sci.* **2000**, *113 Pt 16*, 2909–2921. [[CrossRef](#)] [[PubMed](#)]
64. Iyer, V.; Pumiglia, K.; DiPersio, C.M. Alpha3beta1 integrin regulates MMP-9 mRNA stability in immortalized keratinocytes: A novel mechanism of integrin-mediated MMP gene expression. *J. Cell Sci.* **2005**, *118*, 1185–1195. [[CrossRef](#)]